AN INVESTIGATIVE STUDY OF THE INTERFACE HEAT TRANSFER COEFFICIENT FOR FE MODELLING OF HIGH SPEED MACHINING

Syed Amir Iqbal[1], Paul T Mativenga[2], Mohammad A Sheikh[2]

ABSTRACT

This paper is concerned with the development of an experimental setup and Finite Element (FE) modelling of dry sliding of metals to estimate interface heat transfer coefficient. Heat transfer between the chip, the tool, and the environment during the metal machining process has an impact on temperatures, wear mechanisms and hence on tool-life and on the accuracy of the machined component. For modelling of the metal machining process, the interface heat transfer coefficient is an important input parameter to quantify the transfer of heat between the chip and the tool and to accurately predict the temperature distribution within the cutting tool. In previous studies involving FE analysis of metal machining process, the heat transfer coefficient has been assumed to be between 10-500 kW/m^2 ^{o}C (0.49-24.5 BTU/sec/ft^2/^{o}F), with a background from metal forming processes (especially forging). Based on the operating characteristics, metal forming and machining processes are different in nature. Hence there was a need to develop a procedure close to metal machining process, to estimate this parameter in order to increase the reliability of FE models. To this end, an experimental setup was developed, in which an uncoated cemented carbide pin was rubbed against a steel workpiece while the later was rotated at speeds similar to the cutting tests. This modified pin-on-disc set-up was equipped with temperature and force monitoring equipment. A FE model was constructed for heat generation and frictional contact. The experimental and modelling results of the dry sliding process yield the interface heat transfer coefficient for a range of rubbing speeds.

Keywords: High Speed Machining, frictional contact, Interface heat transfer coefficient

1. INTRODUCTION

The work done to plastically deform and shear away workpiece material during the machining process is largely converted into heat. O'Sullivan D, Cotterell M. Temperature Measurement in Single Point Turning. J Materials Processing Technology 2001;118:301-308. This heat energy increases the temperatures of the chip, the tool and the machined surface. A very small amount of this heat energy is dissipated to the environment. The second largest source of heat generation during the machining process for cases where undeformed chip thickness is far greater than the tool edge radius has been identified as the frictional heat source in the secondary deformation zone. As a result, heat flows from the chip to the tool rake face and a thermal contact exists between these contacting surfaces. This heat transfer between the chip, the tool and the environment has an impact

[1]*Department of Industrial and Manufacturing Engineering, NED University of Engineering & Technology, Karachi, Pakistan, Ph. +92-21-9261261-68, Fax. +92-21-9261255, Email: syed_a_iqbal@yahoo.com,*

[2]*Manufacturing and Laser processing Group, School of Mechanical, Aerospace and Civil Engineering, The University of Manchester, Manchester, UK*

(Reproduced with the permission of Proceedings of the Institution of Mechanical Engineers, Part B: Journal of Engineering Manufacture)

Syed Amir Iqbal received his PhD in modeling of High Speed Machining Process from the University of Manchester in 2008, under the joint supervision of Drs Mativenga and Sheikh. He has published articles on tool-chip contact and interface phenomena at high cutting speeds.

Paul T Mativenga received his PhD in High speed machining from The University of Liverpool in 2001. Since 2002, he has held a lecturing post at UMIST and then subsequently the University of Manchester. He leads a large research group investigating thin film tool coatings, micromachining and high speed machining and has published widely on these topics. He is a Principal Investigator on an active DTI/EPSRC extend life micro tooling project.

Mohammad A Sheikh received his MSc and PhD from University of Sheffield in 1978-1983. He is Currently a senior Lecturer in the University of Manchester. He has vast experience in the field of mechanical damage and thermal transport analysis of composites, computer aided modeling of materials in manufacturing, modeling of laser process and machining.

on temperatures, wear mechanisms and hence on tool life and accuracy of the machined surface. The heat transfer at the tool-workpiece interface is commonly assumed to be governed by the interface heat transfer coefficient. The interface heat transfer coefficient *h* can be defined by Eq. 1 as shown below:

$$h = \frac{q}{\Delta T} \tag{1}$$

where q is the average heat flow across the interface and ΔT is the temperature drop. It has been established that interface heat transfer coefficient is a function of several parameters, the dominant ones being contact pressure, interstitial materials, macro and micro geometries of the contacting surfaces, temperature and the type of lubricant or containment and its thickness [2].

For the FE modelling of metal machining processes, the boundary conditions at the tool-chip interface are usually formulated in terms of the interface heat transfer coefficient. Thus, the interface heat transfer coefficient is an important input parameter to quantify the transfer of heat between the chip and the tool, and to accurately predict the temperature distribution within the cutting tool. In all the previous work on FE modelling of metal machining process, the numerical values used for defining interface thermal boundary condition were taken from metal forming processes (mostly metal forging). A discussion is presented in this paper regarding the differences in the nature and operating characteristics of machining and forging processes. It is concluded from this discussion that there is a need to develop a procedure close to metal machining process, to estimate this parameter in order to increase the reliability of FE models. Due to experimental difficulties in measuring temperature at the tool chip interface, a new method for estimating values of interface heat transfer coefficient is presented. It is based on a simplified setup of two body heat transfer with the amount of heat generated in the rubbing process depending on the rotational speed. The interface heat transfer coefficient for this sliding contact scenario is predicted by using FE modelling approach.

2. EXISTING SCENARIO FOR INTERFACE HEAT TRANSFER COEFFICIENT VALUES IN MACHINING SIMULATIONS

In the application of interface heat transfer coefficient to the chip formation simulations, very high values of '*h*' have been used based on the assumption of perfect contact. Yen et al. [3] used a very high value (value not mentioned) of interface heat transfer coefficient to study the effect of tool geometry on orthogonal machining process, assuming perfect contact between the chip and the tool. In another study, Yen et al. [4] again used a very high value of interface heat transfer coefficient (value not reported) to model tool wear in orthogonal machining, again for perfect contact. To simulate orthogonal machining process using coated tools, again assuming perfect thermal contact between the tool and the chip, Yen et al. [5] used a value of 100 $kW/m^2\,^oC$ (4.89 $BTU/sec/ft^2/^oF$) for the interface heat transfer coefficient. The workpiece material used was AISI 1045 steel with tungsten carbide tool, coated with different coatings at a cutting speed of 220 m/min (722 ft/min). Klocke et al. [6] also assumed a very high value of interface heat transfer coefficient between the tool and the chip for orthogonal machining of AISI 1045 steel with a ceramic tool at ultra high

Table 1. Summary of Interface Heat transfer coefficient values used for machining simulation

Researcher	Workpiece material	Tool material	h(kW/m^2 ^{o}C)
Yen et al [3]	AISI 1020	Uncoated WC	**
Yen et al [4]	AISI 1045	Tic/Al_2O_3/Tin coated WC	100
Yen et al [5]	AISI 1045	Uncoated WC	100
Klocke et al [6]	AISI 1045	SiC-Ceramic	**
Ozel [8]	LCFCS	Uncoated WC	100
Xie et al [9]	AISI 1045	Uncoated WC	10
Miguelez et al [10]	42CrMo4	Uncoated WC	**
Coelho et al [11]	AISI 4340	PCBN	500
Arrazola et al [12]	AISI 4140	ISO P10 carbide	100000

***Value not reported. Perfect contact was assumed between tool and workpiece.*

cutting speed. Their assumption was based on experimental results for temperature and chip surface in the secondary deformation zone. Marusich and Ortiz [7] used the first law of thermodynamics to account for thermal effects produced during the cutting process. The heat generated at the sliding contact was considered to be a function of the difference in the velocity across the contact. This was divided proportionately between the tool and the chip based on their thermal conductivity, density and heat capacity values. Ozel [8] used a value of 100 kW/m^2 ^{o}C (4.89 BTU/sec/ft^2/^{o}F) as interface heat transfer coefficient for studying the effect of different friction models on the output of orthogonal machining process. Xie et al. [9] simulated 2D tool wear in turning of AISI 1045 steel with an uncoated tungsten carbide tool at a cutting speed of 300 m/min. Their FE model used a value of 10 kW/m^2 ^{o}C (0.49 BTU/sec/ft^2/^{o}F) to define the gap conductance at the tool-chip interface. Miguelez et al. [10] simulated orthogonal metal cutting process by using two different numerical approaches, i.e. Lagrangian and Arbitrary Lagrangian Eulerian, with different chip separation criteria. Here, the relation defining the heat flux crossing the tool-chip interface was directly related to interface gap conductance. The value of gap conductance was again assumed to be very high for perfect heat transfer between the tool and the chip. Coelho et al. [11] simulated orthogonal metal cutting process using Arbitrary Lagrangian Eulerian approach for AISI 4340 steel as workpiece and PCBN as cutting tool using finishing cutting parameters. A gap conductance value of 500 kW/m^2 ^{o}C (24.5 BTU/sec/ft^2/^{o}F) was used considering perfect heat transfer. Arrazola et al. [12] simulated the orthogonal metal cutting process, for the study of serrated chip formation during simulation of metal cutting process using Arbitrary Lagrangian Eulerian approach. They analysed the sensitivity of serrated chip prediction to the numerical and cutting parameters using AISI 4140 steel as workpiece and uncoated ISO P10 grade carbide as cutting tool. A gap conductance value of 10^5 kW/m^2 ^{o}C (4.89 BTU/sec/ft^2/^{o}F) was used considering heat transfer with perfect thermal contact. **Table 1** summarizes the values of the interface heat transfer coefficients used for the simulation of metal machining process.

3. METHODS USED PREVIOUSLY FOR THE ESTIMATION OF INTERFACE HEAT TRANSFER COEFFICIENT

Many different approaches have been used to estimate interface heat transfer coefficient. However, most of the previous work focused on hot and cold forming processes rather than machining. For these (forming) processes, analytical, experimental and numerical approaches were used to define and estimate heat transfer between solids under sliding contact. Most of the analytical studies estimated the contact temperature by considering two semi infinite solids under steady-state conditions and assuming a band, circular or elliptic shaped contact, with applications in strip rolling [13-16]. Bos and Moes [17] used asymptotic solutions for circular and semi-elliptic band contact to analyse heat partitioning problem by matching surface temperatures. Their solutions covered a wide range of Peclet numbers. Bauzin and Laraqi [18] used the least square method to estimate the heat generated, thermal contact conductance and heat partition coefficient simultaneously.

The experimental work has mainly focused on the determination of heat partition and thermal contact conductance. Berry and Barber [19] developed a symmetric cylinder on cylinder experimental setup to study the division of frictional heat in sliding contact. They concluded that oxide films have an appreciable effect on microscopic thermal resistance. Lestyan et al. [20] developed a test rig to perform dry sliding of alumina-steel pair to analyse contact and temperatures developed in the

contact region. Some experimental studies, for determining the thermal contact conductance, were conducted using devices which contained two tools or two tools with a workpiece sandwiched between them [21-24]. These experiments were followed by an assessment of the interface heat transfer coefficient whilst the specimen deformed plastically. Another method was based on the solution of an inverse problem; a sequential inverse method was used to determine the thermal contact conductance in metal forming processes [25]. A further method was based on matching the experimentally measured temperature with analytical and/or numerical solutions for various values of '*h*'. The interface heat transfer coefficient was taken to be the value which provided the best match between simulation and experimental results [23-24,26].

4. EFFECT OF OPERATING PARAMETERS ON '*H*' VALUE IN FORGING PROCESSES

As mentioned earlier, the interface heat transfer coefficient is influenced by several operating parameters such as pressure, macro and micro geometries of the contacting surfaces and temperature. In this section, the effects of these operating parameters on the interface heat transfer coefficient are discussed.

4.1 Effect of Pressure

During the forging process, the pressure applied by closing the die largely influences the interface heat transfer coefficient. Semiatin et al. [21] reported an experimental and analytical technique for the determination of interface heat transfer coefficient for non-isothermal bulk forming process. Two instrumented dies were heated to different temperatures and brought together under varying pressure levels. A one dimensional analysis and a finite difference model were used in the evaluation of interface heat transfer coefficient. They concluded that in the absence of deformation, the heat transfer coefficient increases with increasing interface pressure. Above a threshold pressure, the interface heat transfer coefficient becomes insensitive to the forging pressure. Similar results were reported by Lambert et al. [27] and Lambert and Fletcher [28]. They produced design graphs for the thermal contact conductance for three major aerospace alloys, with pressure up to 100 MPa (7.25 tons/in^2) and temperature of 300 ^{o}K (80 ^{o}F). Hu et al. [29] also reported a similar trend of increase in heat transfer coefficient with increasing interface pressure, for the forging of Ti6Al4V alloy. The temperature and pressure taken in their study were 920 ^{o}C (1688 ^{o}F) and 500 MPa (36.25 tons/in^2), respectively.

4.2 Effect of Temperature

Malinowski et al. [22] studied heat transfer coefficient as a function of temperature and pressure. They used temperature measurement in two dies in contact and employed FE method to determine the interface heat transfer coefficient. They developed an empirical relationship giving interface heat transfer coefficient as a function of time, temperature and interfacial pressure. However, they neglected the heat generation within the workpiece. They concluded that interface heat transfer coefficient was not as strongly dependent on temperature as on pressure.

4.3 Effect of Interface Friction

Burte et al. [24] studied the coupling between heat transfer coefficient and friction during hot forging process. They analysed the data from ring compression tests combined with generation of heat transfer coefficient and friction shear factor calibration curves derived from FE simulations. They reported that the effect of friction shear factor on heat transfer coefficient was small. Their simulation results and corroborating experimental observations led to the conjecture that heat transfer and friction may be decoupled in the analysis of metal working process for similar geometry and processing conditions.

4.4 Effect of Deformation Speed

Semiatin et al. [21] deduced from a ring compression test, involving both deformation and heat transfer, that the heat transfer coefficient increased with deformation rate. Similar trend was also reported by Hu et al. [29], with strain rates of 0.125 s^{-1} and 1.0 s^{-1} and with higher values of pressure and temperature as compared to ones used by Semiatin et al. [21]. This can be explained by the fact that at high deformation rates, most of heat transfer occurs simultaneously with the process which tends to smooth interface asperities. On the contrary at low deformation rates, heat transfer occurs prior to large deformation.

4.5 Effect of Surface Roughness

Lambert and Fletcher [28] studied the effect of a non-flat, rough and metallic coated surface on thermal contact conductance. They concluded that the interface heat transfer coefficient increased with increasing roughness of contacting surfaces. Rough surfaces add more resistance to the transfer of heat. Similarly in the case of lubricants and coatings, applied to the interface during forging process to reduce interfacial friction, also adds to the resistance to heat transfer between contacting surfaces, thereby resulting in a reduction in interface heat transfer coefficient.

5. COMPARISON BETWEEN MACHINING AND FORGING PROCESS: OPERATING CHARACTERISTICS

Based on the discussion presented earlier, there are some contrasting factors related to the nature of bulk forming and machining. In the case of hot bulk forming process, the interface heat transfer coefficient is influenced by rate of deformation encountered during the process. The maximum strain rates involved in forging processes are of the order of 10^3 s^{-1} [30] and are relatively low as compared to the machining process. The deformation rates involved during the machining processes, on the other hand, are very high typically of the order of 10^6 s^{-1} [31]. Similarly the difference in temperatures involved in these processes is very high. Kalpakjian [30] reported that homologous temperature (ratio of operating temperature to the melt temperature) for forging processes ranges between 16%-70%, whereas for machining process it can go up to 90%, i.e. closer to the melt temperature and higher as compared to forging processes.

The contact area is also a critical issue in this comparison, as it provides a passage for heat transfer between mating surfaces. In the case of metal machining, the contact area between the tool and the chip is small and does not vary substantially during the machining process. In machining of AISI 1045 steel with uncoated cemented carbide, the contact area decreases with increasing cutting speed for cutting speed up to 900 m/min (2953 feet/min) [32]. However, in the case of metal forging (considering the case of upset forging), the contact area increases substantially with increasing percentage reduction in height during the forming process. Also, the nature of contact in the two processes under consideration is different. In the case of forging, mating components remains in contact during the whole process whereas, in the case of machining, fresh workpiece material comes in contact continuously with the tool rake face. For the latter case, it is necessary to develop an experimental setup for the determination of interface heat transfer coefficient suitable for the machining process.

6. RUBBING EXPERIMENTS

An experimental setup adapted from that proposed by Lancaster [33] and Olsson [34], for the study of wear was used in this case to study the heat transfer problem. Rubbing tests were performed, where the end surface of a cylindrical pin made of tool material was pressed against the end surface of a rotating workpiece. For these tests, a pin of 2.5 mm (0.1 in.) diameter and 15 mm (0.6 in) length was made of cemented tungsten carbide (same grade as ISO P10- P20 cutting tool). The end surface of the pin was ground to a negative relief angle (approximately 5°- 10°) so as to avoid chip formation. The mass of the pin was measured using a precision electronic balance to calculate the amount of weight loss during the rubbing process. The pin was assembled on the tool holder in order to regulate its radial position compared to the thickness of the cylindrical workpiece. The tool holder was then mounted on a Kistler 3 component piezoelectric dynamometer to measure forces. An AISI 1045 workpiece of a hollow cylindrical shape with a wall thickness of 2.5 mm (0.1 in.) was used. The rubbing experiments were performed at the rubbing speeds of 56, 139, 195, 279, 391, 441, 558 and 776 m/min (2.5 feet/min), on a lathe machine equipped with an infrared thermal imaging camera and a force dynamometer. The rubbing time was set to one minute for all rotational speeds in order to achieve a steady state temperature in the pin and the experiments were repeated three times. The experimental setup is shown in **Figures 1**-**2**. The temperatures were measured using an infrared thermal imager FLIR ThermalCAM_ SC3000. This system is a long-wave and self-cooling analysis system with a cool down time of less than six minutes. The accompanied software package allows detailed analysis of highly dynamic objects and events typically found in metal machining applications. The thermal imaging camera has a temperature range of 20 ^{o}C (68^{o}F) to 2000 ^{o}C (3632 ^{o}F) with an accuracy of ±2 ^{o}C (36 ^{o}F) for measurement range above 150 ^{o}C (302 ^{o}F) . This camera can capture and store thermal images and data at high rates (up to 750 Hz for PAL and 900 Hz for NTSC format) with the ThermaCAM Researcher^{TM} 2.8 package. Complete technical specifications of the thermal imaging system are given in **Table 2**. **Figure 2** shows the position of thermal imaging camera in the experimental setup. The camera was positioned at a distance of 45 cm (18 in.) from the pin. The

stored images were recalled and analysed by using the available software. When placed on the image the cursor gave the temperature value at the required points. For the rubbing time specified, the pin acquired a uniform temperature in the portion extended from the holder. The real temperature of an object depends strongly on the emissivity of the material, which is of particular concern when a thermal imaging camera is used. An accurate calibration of the thermographic system was carried out to find the emissivity value of the rubbing pin material (uncoated cemented carbide, ISO P20 grade). Samples were heated to temperatures ranging from 100 to 900 ^{o}C (212 to 1652 ^{o}F) in an oven. A thermocouple-infrared pyrometer arrangement was used to read the temperature of the pin, and the emissivity adjusted until the temperature reading of the pyrometer matched a thermocouple reading. The average thermal emissivity of the uncoated cemented carbide pin was found to be 0.55 at 700 ^{o}C (1292 ^{o}F) .

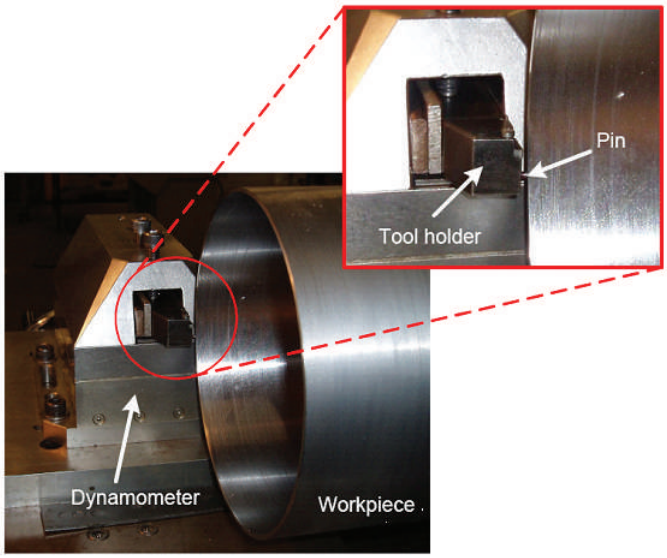

Figure 1. Experimental setup for the pin rubbing tests

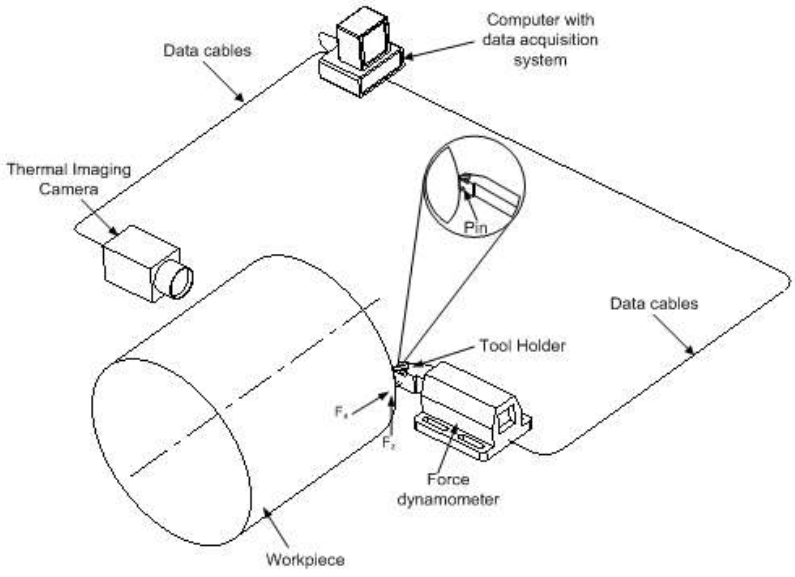

Figure 2. Schematic representation of the experimental setup for the pin rubbing test (showing position of thermal imaging camera)

Table 2. Technical specifications of FLIR system IR thermal imaging camera

IR detector	Quantum well IR photodetector (QWIP)
Spectral range	8-9 μm
Image frequency	50/60 Hz non-interlaced (standard), up to 750/900 Hz (optional and with Researcher HS option)
Thermal sensitivity	20 mK at 30 °C
Temperature range	-20 °C to +2000°C
Accuracy	±1°C (for measurement ranges up to +150 °C) ±2°C (for measurement ranges above +150 °C)
Spatial resolution	1.1 mrad
Pixel per image	320 x 240
Zoom factor	4 x
File format	14-bit radiometric IR digital image (*.IMG) 8-bit standard bitmap(*.BMP)

7. EXPERIMENTAL RESULTS AND DISCUSSIONS

The experimental results are presented in **Figures 3, 5** and **7**. Each data point on these graphs was calculated from measurement of three rubbing tests, shown with corresponding variation in data. **Figure 3** shows the variation of coefficient of friction with rubbing speed. This was calculated from the forces measured during the rubbing process. It shows an overall decreasing trend with increasing rotating speed, similar to the results of other cutting experiments . However, the numerical values of the friction coefficient obtained from these rubbing tests are lower as compared to the previously reported values of cutting experiments for a similar range of speeds . This could be explained by the absence of any sticking in the rubbing tests as compared to the cutting experiments. **Figure 4** shows the variation of maximum temperature measured at a specified location on the pin, with respect to time. Initially there are a few spikes of high temperature (due to the chip formation) but soon afterwards the temperature becomes steady. **Figure 5** shows the variation of pin temperature with rubbing speed. The pin temperature rises sharply in the speed range of 195 to 558 m/min but then stabilizes after that speed in the temperature range of 700 °C to 900 °C (1292 to 1652 °F) . This can be explained in the context of the variation of thermal conductivity of uncoated cemented tungsten carbide. Child et al. reported that the thermal conductivity of ISO P grade uncoated cemented tungsten carbide decreases with increasing temperature (**Figure 6**). This can account for the flatter slope of pin temperature curve at high speeds. The variation of pin wear with rubbing speed is shown in **Figure 7**. Initially the pin material loss is low up to a rubbing speed of 279 m/min (915 ft/min) but it rises sharply at a rubbing speed of 391 m/min (1283 ft/min). It then drops slightly at a rubbing speed of 441 m/min (1447 ft/min) but increases again at a steady rate. It should be noted that the variation in pin temperature and pin weight loss with rubbing speed follow a similar trend. **Figure 8** shows that pressure is approximately constant for all the rubbing speeds, except for the lowest speed. It is evident from the results presented in **Figure 3, 5** and **7**, that there is a marked transition in their behaviour. There are three regions which can be identified for all three variables; Region–I, for speed less than 200 m/min (656 ft/min), region-II, for speed greater than 200 m/min (656 ft/min) and less than 600 m/min (1969 ft/min), and region-III, for speeds greater than 600 m/min (1969 ft/min). For rubbing speed less than and equal to 200 m/min (656 ft/min) (region-I), the loss of pin mass is negligible. For rubbing speed interval of 200-600 m/min (656-1969 ft/min), the loss of pin mass is very high. Similarly temperature rises sharply in regions I and II but stabilises in region III. Correspondingly the coefficient of friction decreases in these two regions i.e. in regions I and II and stabilises in region III. In the next section a FE model of the pin rubbing setup will be discussed. The scheme followed is to vary the interface gap conductance to match the experimental pin temperature.

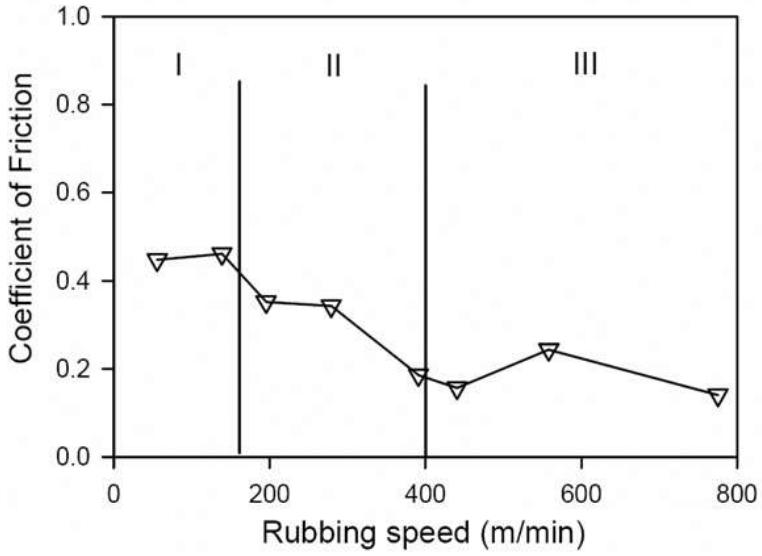

Figure 3. Variation of coefficient of friction with cutting speed

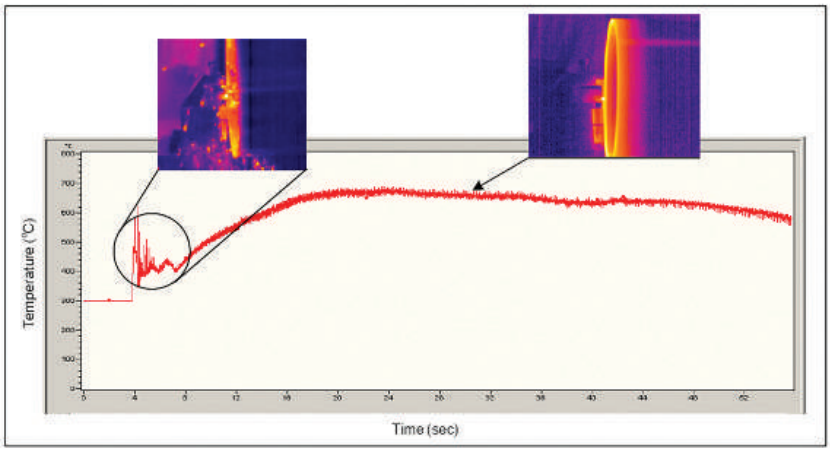

Figure 4. Maximum pin temperature measured during the rubbing process, using the thermal imaging camera

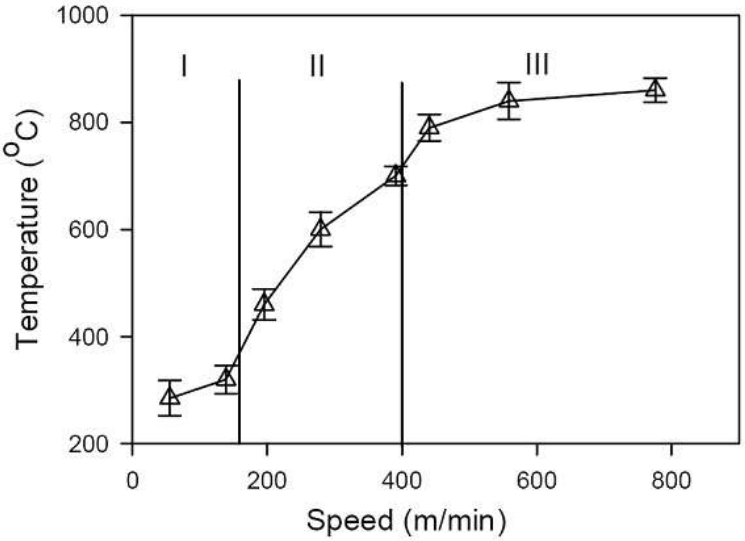

Figure 5. Variation of pin temperature with cutting speed

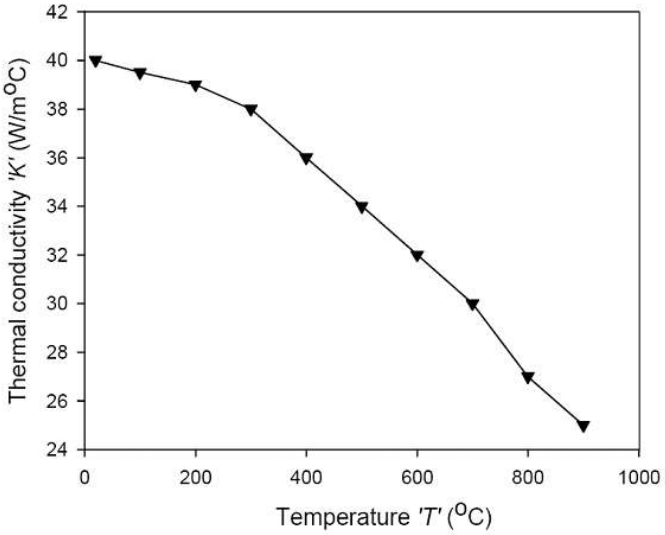

Figure 6. Variation of thermal conductivity with temperature for P20 carbide [36

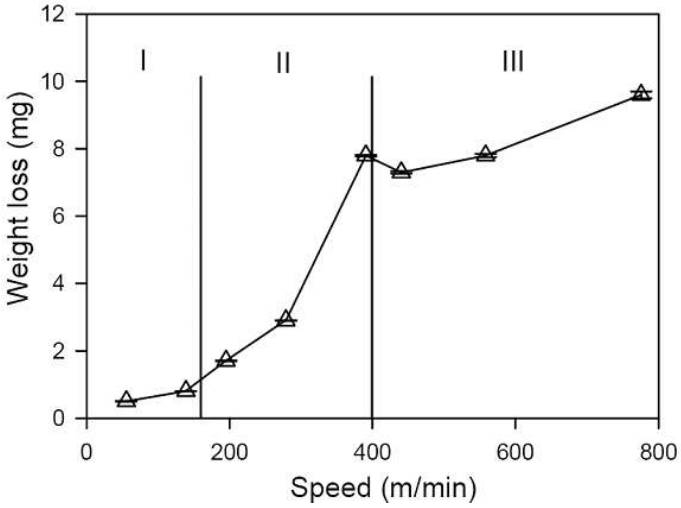

Figure 7. Variation of weight loss of pin with cutting speed

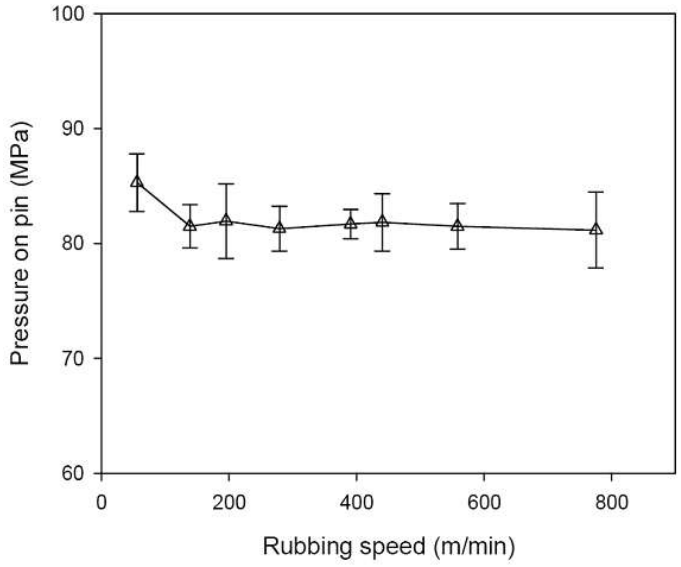

Figure 8. Variation of pressure applied on the pin at different rubbing speeds

8. FE MODELLING

In order to numerically simulate the rubbing process, a commercial FE package ABAQUS/Explicit was used. An FE model was developed and the simulations were run with conditions similar to the experiments. As the problem involved a number of strongly interacting mechanical and thermal processes like friction, temperature and wear, a coupled thermo-mechanical model was developed. The heat produced by friction (mechanical work) acts as a source for the thermal problem. The work presented here is based on the rubbing process only, i.e. wear is neglected. This is justifiable because the volume of material removed (in milligrams) from the pin during rubbing process was very low compared to the advanced wear processes involved in real machining. The FE model used for simulating the rubbing process is shown in **Figure 9**. In this model, the carbide pin was held stationary, while the AISI 1045 steel workpiece revolves with a rubbing speed ranging from 56 to 776 m/min (184 to 2546 ft/min). A graded mesh was used for both the pin and workpiece, with higher mesh density in the interface zone. With reference to **Figure 9**, the boundary conditions used for the model are defined as follows: the contact surfaces of the pin and the workpiece were assumed to be smooth and in perfect contact. The contact between the pin and workpiece was evaluated by using an optical microscope to examine the pin face. The wear marking on the pin showed full contact. The exterior boundaries are exposed to still air except the contacting regions of the pin and the workpiece. For exterior regions, the convective heat transfer coefficient is assumed to be h_∞ = 0.02 kW/m^2 ^{o}C (9.7 x 10^{-4} BTU/sec/ft^2/^{o}F) . Any heat loss due to radiation is neglected. The whole model was set at room temperature. The experimental values of coefficient of friction (shown in **Figure 3**) are used at the interface of the pin and the counter material for each rubbing speed. The material properties used for the pin and the workpiece materials are listed in **Table 3**. In the application of contact formulation for FE model, the carbide pin is taken as the 'slave' and the AISI 1045 steel workpiece as the 'master'. Heat partition is an important issue in sliding contact of two bodies for which several approaches have been followed by different researchers . For FE model developed for this study, the heat partition ratio at the interface between the pin and the workpiece is given mathematically by Eq. 2.

$$\frac{H_1}{H_2} = \frac{\sqrt{\rho_1 C_1 K_1}}{\sqrt{\rho_2 C_2 K_2}} \qquad (2)$$

where H is the heat partition, is the density (kg/m^3), K is the thermal conductivity (W/m^2 ^{o}C) and C is the specific heat capacity (J/m^2 ^{o}C). Subscripts 1 and 2 represent the pin and workpiece materials respectively. Temperature dependent data, given in **Table 3**, was used to evaluate Eq. 2.

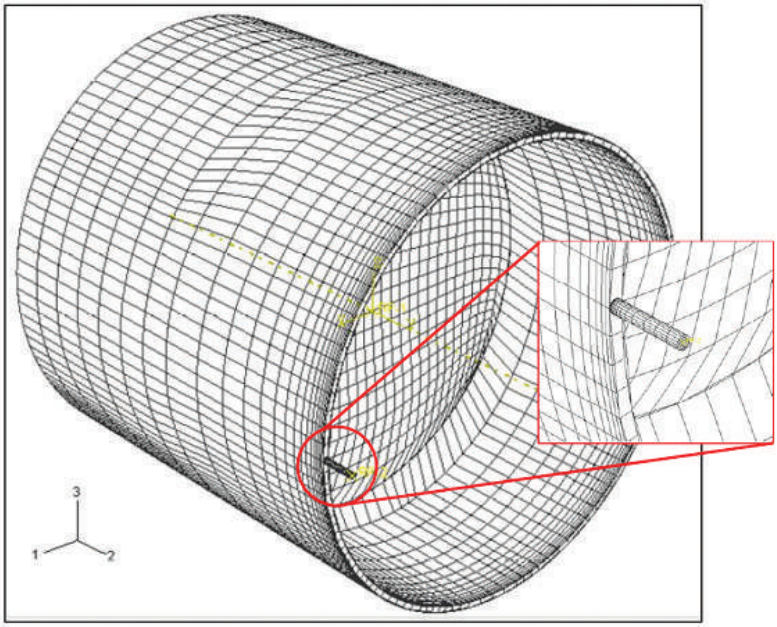

Figure 9. FE model of the rubbing process

Table 3. Material properties of Pin and counter material [37]

Thermal/ mechanical properties	**Tool : Uncoated cemented carbide***	Poisson's ratio		0.3											
		Thermal Expansion	^oC	20-800											
			$^oC\ ^{-1}(x10^{-06})$	6.3											
		Heat Capacity	^oC	240	450	640	695								
			$N.mm^{-2}.^oC^{-1}$	3.66	3.8	4.31	5.1								
		Modulus of elasticity	^oC	20	200	300	500	700							
			GPa	520	509	494	487	487							
		Thermal Conductivity	^oC	20	100	200	300	400	500	600	700	800	900		
			$W.m^{-1}.^oC^{-1}$	40	39.5	39	38	36	34	32	30	27	25		
	Workpiece: AISI 1045	Poisson's ratio		0.3											
		Thermal Expansion	^oC	20	200	400	600								
			GPa	215	210	165	160								
		Heat Capacity	^oC	100	200	300	400	500	600	700					
			$^oC\ ^{-1}(x10^{-05})$	1.12	1.19	1.27	1.35	1.41	1.45	1.46					
		Modulus of elasticity	^oC	25	125	325	525	725	825	875	925	975			
			$N.mm^{-2}.^oC^{-1}$	3.66	3.8	4.31	5.1	8.76	8.27	7.48	6.04	5.64			
		Thermal Conductivity	^oC	25	100	300	500	700	800	900	950	1000	1050	1100	1150
			$W.m^{-1}.^oC^{-1}$	45	42.5	38	34.5	29	28	24	23	23	24	26	27

* Room temperature properties are provided by Sandvik Coromant. For temperature dependent properties, data from [36] is followed.

The interface heat transfer coefficient between the pin and the workpiece is defined in the FE model by gap conductance. This parameter controls the amount of heat flowing through the interface. The strategy used here was to vary the value of gap conductance in the simulation and match the simulated temperatures on the pin with experimental values at the same location. For the matched temperatures, the gap conductance value used in the simulation defined the interface heat transfer coefficient. During the rubbing experiments, only a small length of the pin protruded from the tool holder in order to avoid any excessive pin deflection or breakage. Due to this short protruded length of the pin, the measured temperature of the pin was almost uniform.

9. NUMERICAL RESULTS

A series of simulations for all the rubbing speeds ranging from 56 to 776 m/min were carried out. The interface heat transfer coefficient values for these speeds, following the procedure outlined in the previous section, are shown in **Figure 10**. These results show that the value of interface heat transfer coefficient is initially high (300 $kW/m^2\ ^oC$ (14.67 $BTU/sec/ft^2/^oF$) for a low rubbing speed of 56 m/min (184 ft/min). The value then reduces to 100 $kW/m^2\ ^oC$ (4.89 $BTU/sec/ft^2/^oF$) at 139 m/min (456 ft/min) and remains constant until the rubbing speed of 279 m/min (915 ft/min). After that, it increases to a value of 150 $kW/m^2\ ^oC$ (7.34 $BTU/sec/ft^2/^oF$) for the rubbing speed of 441 m/min (1447 ft/min) and again decreases to a value of 100 $kW/m^2\ ^oC$ (4.89 $BTU/sec/ft^2/^oF$) at 776 m/min (2546 ft/min). By examining the pin temperatures for this speed range (**Figure 5**), the pin temperature rises steadily before stabilizing for high rubbing speeds (>558 m/min (1831 ft/min)). The pin wear rate shows a direct dependence on the pin temperature (**Figure 5**). As shown in **Figure 8**, the pressure corresponding to the load applied on the pin approximately remains constant except for the very low speed. In this context, by comparing **Figure 5** and **Figure 10**, it is observed that the interface heat transfer coefficient initially shows a decreasing trend with temperature (for the two lowest rubbing speeds) and afterwards it becomes constant for high rubbing speeds. Thus the interface heat transfer coefficient shows a dependence on the temperature for low rubbing speeds (**Figure 11**). For the forging methods, the temperature of both the workpiece and the die are varied for the estimation of interface heat transfer coefficient. Also, heat generated during bulk forming is involved in the process. For the rubbing process on the other hand, both the pin and the workpiece are at surrounding temperature and the source of heat generation is rubbing and sliding only. As mentioned earlier, Malinowski reported that the interface heat transfer coefficient is strongly

dependent on die pressure and not on die temperature. Here, the interface heat transfer coefficient shows a modest dependence on temperature attained during the process. It may be noted that the slight increase in the interface heat transfer coefficient value is for the rubbing speed range of 391–558 m/min (1283-1831 ft/min) which falls under the conventional to high speed machining transition range for AISI 1045 steel . It is also important to note that all the estimated values of interface heat transfer coefficient '*h*' vary between 100 to 300 kW/m^{2}ºC (4.89 to 14.68 BTU/sec/ft^2/ºF). These values fall within the range of assumed values used previously for the simulation of metal machining process (10-500 kW/m^2 ºC) (0.49-24.46 BTU/sec/ft^2/ºF). However, the range is narrower than before. Another important point is that wear of the pin material is not considered in the modelling of rubbing process. This was justifiable because only minute pin wear was recorded (**Figure 7**). Significant pin wear may affect the interface heat transfer coefficient value. However, FE modelling of wear mechanisms is a challenging and ongoing task.

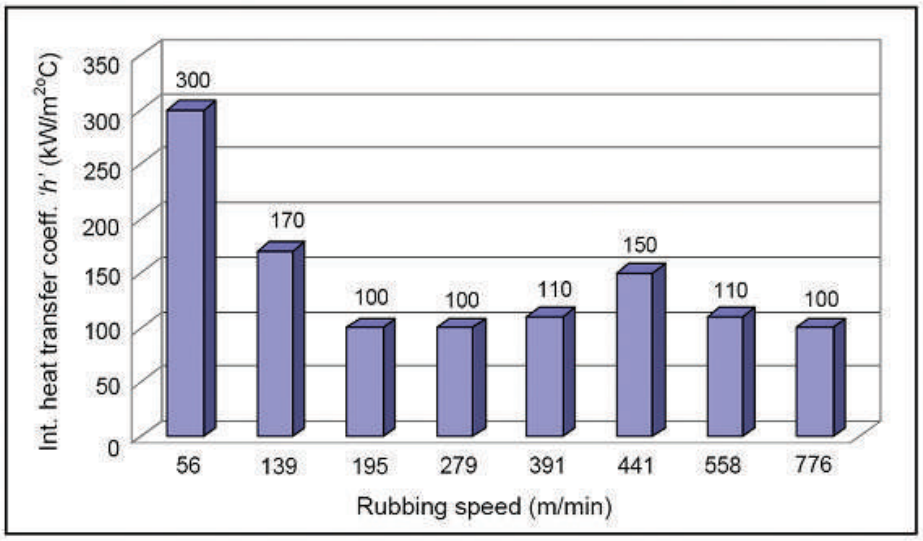

Figure 10. Variation of the interface heat transfer heat coefficient with rubbing speed

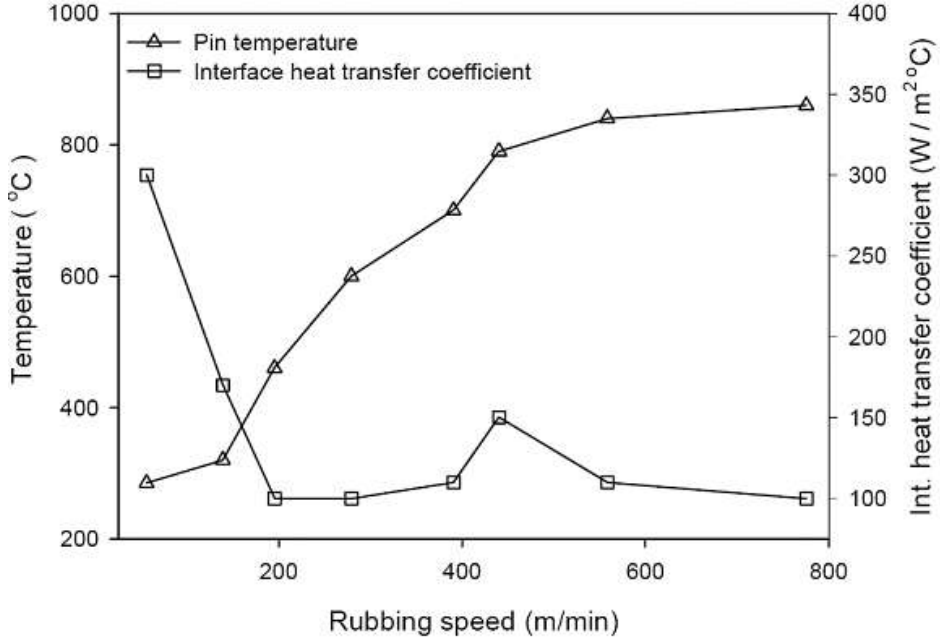

Figure 11. Variation of the pin temperature and interface heat transfer coefficient with rubbing speed

10. CONCLUSIONS

Based on the findings from experimental and modelling results, following conclusions can be drawn:

- Interface heat transfer coefficient is an important parameter which quantifies the amount of heat transferred to the cutting tool in the FE modelling of mechanical machining processes. The resulting temperature distribution in the cutting tool is, in turn important for the modelling of tool wear processes. The present practice is to use interface heat transfer coefficient values estimated from metal forging process, based on the assumption of perfect contact.
- Based on the operating range of strain, strain rate and temperature, the nature of contact in forging and machining processes are dissimilar. An experimental procedure close to the machining process should be used for the estimation of interface heat transfer coefficient.
- A new method based on rubbing of a carbide pin of material similar to the cutting tool with AISI1045 steel as counter material was employed. In addition, an FE model of the rubbing process was developed for the estimation of interface heat transfer coefficient for a wide range of rubbing speeds.
- Results show that the estimated interface heat transfer coefficient decreases at low rubbing speeds and then becomes approximately constant for high rubbing speeds. At these low rubbing speeds, the estimated values show a dependence on temperature.
- All the estimated values of interface heat transfer coefficient '*h*' lie between 100–300 $kW/m^2\,^oC$ (4.89-14.68 $BTU/sec/ft^2/^oF$). A majority of cutting speeds can be modelled by using *h* value equal to 100 $kW/m^2\,^oC$ (4.89 $BTU/sec/ft^2/^oF$). Results suggest that assuming '*h*' values lower than 100 $kW/m^2\,^oC$ (4.89 $BTU/sec/ft^2/^oF$) or greater than 300 $kW/m^2\,^oC$ (14.68 $BTU/sec/ft^2/^oF$) would lead to errors in the estimation of thermal fields and chip morphology. Values of 10 $kW/m^2\,^oC$ (4.89 $BTU/sec/ft^2/^oF$), 500 and 100,000 $kW/m^2\,^oC$ (24.46 and 4892 $BTU/sec/ft^2/^oF$) have been assumed by some previous researchers without proper justification.

REFERENCES

1] O'Sullivan D, Cotterell M. Temperature Measurement in Single Point Turning. J Materials Processing Technology 2001;118:301-308.

[2] Madhusudana CV. Thermal Contact Conductance. Springer, Berlin, 1996,. p. 1-23.

[3] Yen Y-C, Jain A, Altan T. A Finite Element Analysis Of Orthogonal Machining Using Different Tool Edge Geometries. J Materials Processing Technology 2004;146:72-81.

[4] Yen Y-C, Sohner J, Lilly B, Altan T. Estimation of Tool Wear In Orthogonal Cutting Using Finite Element Analysis. J Materials Processing Technology 2004;146:82-91.

[5] Yen Y-C, Jain A, Chigurupati P, Wu W-T, Altan T. Computer Simulation Of Orthogonal Metal Cutting Using A Tool With Multiple Coatings. Machining Science and Technology 2004;8(2):305-326.

[6] Klocke F, Raedt H-W, Hoppe S. 2D-FEM Simulation of the Orthogonal High Speed Cutting Process. Machining Science and Technology 2001;5(3):323–340.

[7] Marusich TD, Ortiz M. Modelling and Simulation of High-Speed Machining. J Numerical Methods in Engineering 1995;38:3675 -3694.

[8] Ozel T. The Influence Of Friction Models On Finite Element Simulations Of Machining. J Machine Tools and Manufacture 2006;46(6):518-530.

[9] Xie L-J, Schmidt J, Schmidt C,Biesinger F. 2D FEM Estimate Of Tool Wear In Turning Operation. Wear 2005;258:1479–1490.

[10] Miguelez H, Zaera R, Rusinek A, Moufki A, Molinari A. Numerical Modelling Of Orthogonal Cutting: Influence Of Cutting Conditions And Separation Criterion. Journal De Physique 2006;134:417-422.

[11] Coelho RT, Ng E-G, Elbestawi MA. Tool Wear When Turning AISI 4340 with Coated PCBN Tools Using Finishing Cutting Conditions. J Machine Tools & Manufacture 2007;47:263-272.

[12] Arrazola PJ, Villar A, Ugarte D, Marya S. Serrated Chip Prediction In Finite Element Modelling Of The Chip Formation Process. Machining Science and Technology 2007;11(3):367-390.

[13] Yuen WYD. Heat Conduction In Sliding Solids. J Heat and Mass Transfer 1988;31(3):637-646.

[14] Cameron A, Gordon AN, Symm GT. Contact Temperatures in Rolling/Sliding Surfaces. Proceedings of the Royal Society of London. Series A, Mathematical and Physical Sciences 1965;286(1404):45-61.

[15] Symm GT. Surface Temperature Of Two Rubbing Bodies. J Mechanics and Applied Mathematics, 1967; 20(3): 381-391.

[16] Barber JR. The conduction of heat from sliding solids. J Heat and Mass Transfer 1970;13:857-869.

[17] Bos J, Moes H. Frictional Heating Of Tribological Contacts. Transaction of ASME. J Tribology 1995;117:171-177.

[18] Bauzin J-G, Laraqi N. Simultaneous Estimation Of Frictional Heat Flux And Two Thermal Contact Parameters For Sliding Contact. Numerical heat transfer, Part-A, 2004;45:313-328.

[19] Berry GA, Barber JR. The Division Of Frictional Heat- A Guide To The Nature Of Sliding Contact. Transaction of ASME. J Tribology 1984;106:405-417.

[20] Lestyan Z, Varadi K, Albers A. Contact and Thermal Analysis Of An Alumina-Steel Dry Sliding Friction Pair Conisdering The Surface Roughness. J Machine Tools & Manufacture 2007;40:982-994.

[21] Semiatin SL, Collings EW, Wood VE, Altan T. Determination of the Interface Heat Transfer Coefficient For Non Isothermal Bulk Forming Process. Transactions of the ASME. J Engineering for Industry 1987;109:49-57.

[22] Malinowski Z, Lenard JG, Davies ME. A Study Of The Heat-Transfer Coefficient As A Function Of Temperature And Pressure. J Materials Processing Technology 1994;41:125-142.

[23] Nshama W, Jeswiet J. Evaluation of Temperature And Heat Transfer Conditions At The Metal Forming Interfaces. Annals of CIRP 1995;44(1):201-205.

[24] Burte PR, Yong-Tack I, Altan T, Semiatin SL. Measurements and Analysis Of The Heat Transfer And Friction During Hot Forging. Transactions of the ASME. J Engineering for Industry 1990;112:332-339.

[25] Goizet V, Bourouga B, Bardon JP. Experimental Study Of The Thermal Boundary Conditions At The Workpiece–Die Interface During Hot Forging. In *11th IHTC*. Kyongju, Korea: 1998. Taylor and Francis, London.

[26] Dadras P,Wells WR. Heat Transfer Aspects Of Non-Isothermal Axisymmetric Upset Forging. Transactions of the ASME. J Engineering for Industry 1984;106:187-195.

[27] Lambert MA, Mirmira SR, Fletcher LS. Design Graphs For Thermal Contact Conductance Of Similar And Dissimilar Light Alloys. J Thermophysics and Heat Transfer 2006;20(4):809-816.

[28] Lambert MA, Fletcher LS. Thermal Contact Conductance Of Non Flat, Rough, Metallic Coated Metals. Transactions of the ASME. J Heat Transfer 2002;124:405-412.

[29] Hu ZM, Brooks JW, Dean TA. The Interfacial Heat Transfer Coefficient In Hot Die Forging Of Titanium Alloy. Proc. IMechE Part C: J. Mech. Engg. Sci. 1998;212(6):485-496.

[30] Kalpakjian S. Manufacturing processes for engineering materials. Addison-Wesley/Longman, Menlo park, 3rd ed., 1997. p. 43-102.

[31] Childs THC, Rowe GW. Physics in Metal Cutting. Reports on Progress in Physics 1973;36(3):223-288.

[32] Iqbal SA, Mativenga PT, Sheikh MA. Characterization of the Machining of AISI 1045 Steel over a Wide Range of Cutting Speeds-Part 1: Investigation of Contact Phenomena. Proc. IMechE Part B: J. Engineering Manufacture 2007;221(5):909-916.

[33] Lancaster J. The formation Of Surface Films At The Transition Between Mild And Severe Metallic Wear. Proceedings of Royal Society A 1963;273:466-483.

[34] Olsson M, Soderberg S, Jacobson S, Hogmark S. Simulation of Cutting Tool Wear By A Modified Pin-On-Disc Test. J Machine Tools and Manufacture 1989;29(3):377-390.

[35] Devillez A, Lesko S, Mozerc W. Cutting Tool Crater Wear Measurement With White Light Interferometry. Wear 2004;256(1-2):56-65.

[36] Childs THC, Maekawa K, Obikawa T, Yamane Y. Metal machining: Theory and application. London: Arnold, London, 2000.

[37] Abukhshim NA, Mativenga PT, Sheikh MA. Investigation of Heat Partition In High Speed Turning Of High Strength Alloy Steel. J Machine Tools and Manufacture 2005;45(15):1687-1695.

[38] Gecim B, Winer WO. Transient Temperatures In The Vicinity Of An Asperity Contact. Transactions of the ASME. J Tribology 1985;107:333-342.

[39] Grzesik W, Nieslony P. A Computational Approach To Evaluate Temperature And Heat Partition In Machining With Multilayer Coated Tools. J Machine Tools and Manufacture 2003;43:1311-1317.

[40] Schulz H, Moriwaki T. High Speed Machining. Annals of CIRP 1992;41(2):637-644.